

## Ionic Conductivity of and Raman Spectroscopy Investigation in Binary Oxosalts $(1 - x)\text{AgPO}_3-x\text{Ag}_2\text{SO}_4$ Glasses

J. P. MALUGANI, R. MERCIER, B. FAHYS, AND G. ROBERT

*Laboratoire d'Electrochimie des Solides ERA 810, Faculté des Sciences-La Bouloie, 25030 Besancon Cedex, France*

Received April 1, 1982; in revised form June 21, 1982

$(1 - x)\text{AgPO}_3-x\text{Ag}_2\text{SO}_4$  homogeneous glasses obtained by quenching of a melt of the two salts are pure ionic  $\text{Ag}^+$  conductors. The RT conductivity is increased from  $2.5 \times 10^{-7}$  to  $4 \times 10^{-6}$  ( $\Omega \text{ cm}$ )<sup>-1</sup> when the ratio of  $\text{Ag}_2\text{SO}_4$  is increased from 0 to 0.3. Raman spectroscopy shows that no modifications of the  $(\text{PO}_3)_\infty$  chain skeleton occur by adding  $\text{Ag}_2\text{SO}_4$ . The low-frequency Raman band lying at about  $55 \text{ cm}^{-1}$  is quantitatively correlated to  $\text{Ag}^+$  oscillations, the hopping distance decreasing from 3.0 to  $2.7 \text{ \AA}$  if a jump process between regular  $\text{Ag}^+$  sites is considered.

### 1. Introduction

The use of glassy solid electrolytes in electrochemical devices presents many fundamental as well as technological advantages. Generally vitreous materials have a poor electrical conductivity so they are of restricted practical interest. Kunze (1) was the first to find a vitreous superionic conductor at room temperature. Some similar materials have been discovered, and many of them are silver conductors and contain AgI (2-6). Studies carried out in the laboratory on solid vitreous electrolytes with silver metaphosphate have shown that it is possible to obtain glasses with a high ionic conductivity over a large composition domain by "dissolution" of the silver halide in a support glass having a low ionic conductivity (7, 8).

The substitution of  $\text{AgX}$  by  $\text{Ag}_2\text{SO}_4$  was carried out to make a better definition of the parameters which govern conductivity variations in this type of material. In this paper

we will analyze, within the glass formation region, the structural and electrical properties of the pseudobinary  $\text{AgPO}_3\text{-Ag}_2\text{SO}_4$  system. The results will be compared with the  $\text{AgPO}_3\text{-Ag}_2\text{O}$  glasses.

### 2. Experimental

**2.1 Glass preparation.** The  $(1 - x)\text{AgPO}_3-x\text{Ag}_2\text{SO}_4$  glasses were prepared by melting, followed by a quenching of silver sulfate and silver metaphosphate mixtures; the silver metaphosphate preparation is described elsewhere (2). Fusion was carried out at a temperature close to  $700^\circ\text{C}$  in silica tubes sealed under primary vacuum. The melts were repeatedly stirred and kept at  $700^\circ\text{C}$  for an hour before being rapidly brought to room temperature. The samples of glasses are obtained in the form of cylinders ( $\theta \approx 10 \text{ mm}$  and  $e \approx 5 \text{ mm}$ ) and are then annealed at  $150^\circ\text{C}$ , about  $10\text{-}30^\circ\text{C}$  lower than the glass transition temperature  $T_g$  determined by DTA.

The extent of the glass-forming range was determined by X-ray diffraction patterns, which were nearly structureless; it corresponds to a molar ratio  $x$  less than 0.3; for higher  $\text{Ag}_2\text{SO}_4$  concentrations ( $x > 0.3$ ) an inhomogeneous system appears in which  $\text{Ag}_2\text{SO}_4$  microcrystals are dispersed in the saturated glass.

**2.2 Electrical measurements.** Electrical measurements were usually performed on molded disks covered with evaporated silver or sputtered platinum. The total conductivity was determined under nitrogen atmosphere using a symmetric Ag/glass/Ag cell. Most of the dc-conductivity data were obtained by complex plane analysis in the frequency range  $10^2$ – $10^5$  Hz (9, 10). A dissymmetric Ag/glass/Pt cell was used for the electronic conductivity measurements by Wagner's polarization technique (11). A potential  $E$  lower than the decomposition potential of the electrolyte ( $\Delta e$ ) is applied to this cell, the platinum electrode acting as "blocking" electrode.

**2.3 Raman spectroscopy investigation.** The Raman experiments were performed with a  $90^\circ$  scattering geometry and the 514.5-nm line of a vertically polarized  $\text{Ar}^+$  laser; the laser power was limited to 100 mW on the sample, the scattered light being analyzed by a double holographic grating of a Jobin Yvon HG 25 spectrometer. The polarization measurements were obtained from the intensities of the Stokes Raman lines in the  $I_{\text{VH}}$  and  $I_{\text{VV}}$  configurations ( $\rho = I_{\text{VH}}/I_{\text{VV}}$ ).

The spectra shown in this paper are the reduced spectra  $I_{\text{R}}$  obtained from  $I_{\text{VV}}$  spectra by the transformation  $I_{\text{R}} = \omega I_{\text{VV}} / (1 + n)$ , where  $n$  is the Bose-Einstein term  $1/[\exp(\hbar\omega/kT) - 1]$  (12). This reduced form is particularly convenient to compare low-frequency spectra at different temperatures because the thermal occupation is eliminated so that the reduced intensity can be related to the density of vibrational states and allows quantitative correlations.

Raman line profiles were fitted by mathematical procedures; we used a Lorentz function modulated by a sinusoidal term,

$$I(\bar{\nu}) = B[\cos \Pi(\bar{\nu} - \bar{\nu}_0)/a]^n \cdot K^2/[K^2 + (\bar{\nu} - \bar{\nu}_0)^2],$$

where  $B$  is the maximum amplitude,  $a$  is the line foot broadness,  $\bar{\nu}_0$  is the maximum frequency, and  $K$  the half-width of the Lorentz term. These fittings allow one to display the components of a dissymmetric broad band with the integrated areas  $A$  of each of them.

### 3. Electrical Properties

The Arrhenius plot of the conductivity versus the inverse of temperature for different composition glasses is shown in Fig. 1. In the 25–140°C range the conductivity follows an Arrhenius relation  $\sigma \approx \sigma_0 \exp(-E_c/RT)$ . Both  $\sigma$  conductivity and  $E_c$  activation energy are strongly dependent on the  $\text{Ag}_2\text{SO}_4$  ratio: the conductivity is increased with  $x$ , the higher value being obtained for

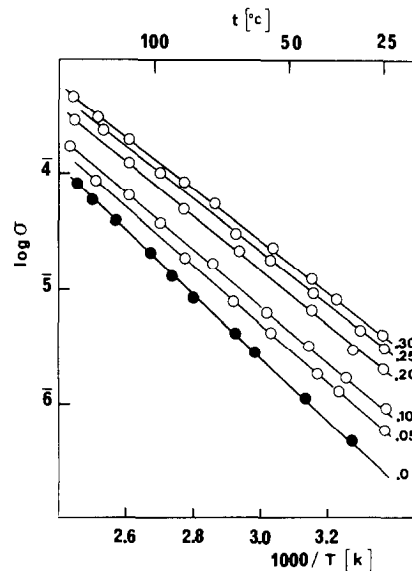


FIG. 1. Temperature dependence of the conductivity  $\sigma$  ( $\Omega^{-1} \cdot \text{cm}^{-1}$ ) of  $(1-x)\text{AgPO}_3-x\text{Ag}_2\text{SO}_4$  glasses.

the saturated glass ( $x = 0.3$ ) ( $\sigma = 4 \times 10^{-6} \Omega^{-1} \text{ cm}^{-1}$  at  $25^\circ\text{C}$ ); for this composition, the activation energy has a minimum value of  $\approx 10$  kcal/mole. On the other hand, the pre-exponential term  $\sigma_0$  remains nearly constant, so the activation energy governs the whole conductivity.

The electronic conductivity value is very low, about  $2 \times 10^{-10} \Omega^{-1} \text{ cm}^{-1}$  at  $25^\circ\text{C}$ ; so the conduction is of an ionic nature and essentially ensured by  $\text{Ag}^+$  cations. The voltage stability window determined by cyclic voltammograms is 1 V, and is limited by the couples  $\text{O}^{2-}/\text{O}_2$  and  $\text{Ag}^+/\text{Ag}$ .

The dissolution of  $\text{Ag}_2\text{SO}_4$  in  $\text{AgPO}_3$  glass gives a large improvement of the ionic conductivity of the host glass; for example, at  $25^\circ\text{C}$ , it is 16 times greater for the saturated glass. To display this enhancement, the  $\sigma_{25^\circ\text{C}}$  dependence on composition is shown in Fig. 2, where, for comparison, the curves we have drawn for  $\text{AgPO}_3\text{-Ag}_2\text{O}$  glasses are reported (13, 14). It must be noticed that the conductivity has the same value for either  $\text{Ag}_2\text{O}$  or  $\text{Ag}_2\text{SO}_4$  at the same concentrations. There is no linear relation between  $\log \sigma$  and  $x$  ratio as in  $\text{AgPO}_3\text{-AgX}$  glasses.

The conductivity seems to be independent of the nature of the silver solute (oxide or sulfate): this behavior, which has been already observed for other glasses (15, 16), suggests that the sulfate anions are inserted

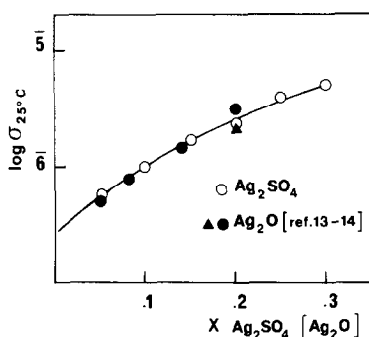


FIG. 2. Composition dependence of  $\sigma_{25^\circ\text{C}}$  ( $\Omega^{-1} \cdot \text{cm}^{-1}$ ) in  $\text{Ag}_2\text{PO}_3\text{-AgSO}_4$  and  $\text{AgPO}_3\text{-Ag}_2\text{O}$  glasses.

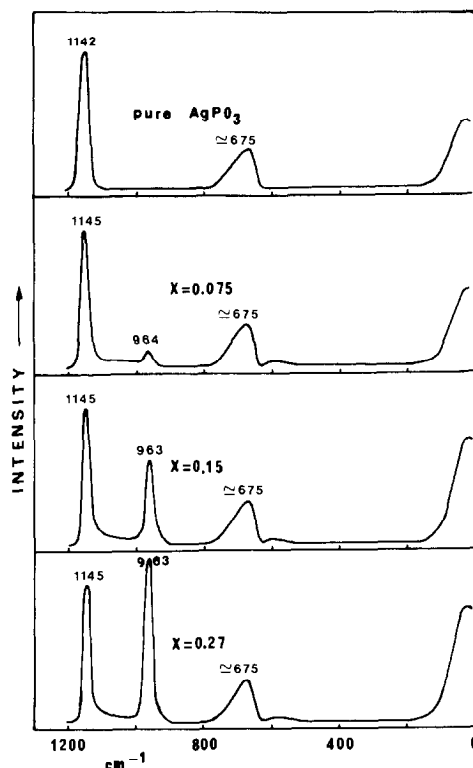


FIG. 3. Raman spectra of  $(1-x)\text{AgPO}_3\text{-(}x\text{)Ag}_2\text{SO}_4$  glasses.

in the same way as the oxide ions in the network. For this reason, we looked at whether there are real structural similarities between these two kinds of glasses; this investigation was performed by *in situ* Raman spectroscopy.

## 4. Raman Investigations

### 4.1. Assignments of the High-Frequency Spectra ( $\bar{\nu} > 200 \text{ cm}^{-1}$ )

The following discussion is limited to the three bands appearing very distinctly at about 700, 965, and 1140  $\text{cm}^{-1}$  (Fig. 3); some other broad and weak bands can also be observed but they are not interesting for our purpose. The polarization measurements ( $\rho = I_{\text{VH}}/I_{\text{VV}}$ ) show that these three main bands are very polarized ( $\rho < 0.1$ ) and thus correspond to the symmetric modes of

high-symmetry species ( $\text{SO}_4$  and  $\text{PO}_4$  tetrahedra). The reference spectra are indeed those of the  $\text{Ag}_2\text{SO}_4$  and  $\text{AgPO}_3$  crystalline compounds.

—Polycrystalline  $\text{Ag}_2\text{SO}_4$  is characterized by one sharp and strong line at  $975\text{ cm}^{-1}$  ( $\nu_1\text{SO}_4$ ) and three weaker lines at  $1180\text{ cm}^{-1}$  ( $\nu_3\text{SO}_4$ ),  $600\text{ cm}^{-1}$  ( $\nu_2\text{SO}_4$ ), and  $450\text{ cm}^{-1}$  ( $\nu_4\text{SO}_4$ ).

—The infinite chains  $(\text{PO}_3)_n$  in crystalline  $\text{AgPO}_3$  (17) give rise to two strong lines at  $1150\text{ cm}^{-1}$  ( $\nu_3\text{PO}_2$ ) and  $720\text{ cm}^{-1}$  ( $\nu_s\text{P-O-P}$ ) and also to weaker bands.

In  $\text{AgPO}_3$  glass, two bands are predominant in the Raman spectrum; the  $1145\text{-cm}^{-1}$  band is sharp (half-width  $\approx 15\text{ cm}^{-1}$ ) and is related to the  $\text{PO}_2$  stretching mode, while the  $720\text{-cm}^{-1}$  band is very broad and dissymmetric; this dissymmetry probably arises from twisted or balled chains, the skeleton POP mode being very sensitive to the configuration of successive linked  $\text{PO}_4$  tetrahedra. It must be underlined that this  $\text{AgPO}_3$  glass spectrum is very similar to that of the  $\text{MPO}_3$  alkaline glass ( $M = \text{Na}, \text{Li}$ ) (18–21), the substitution of cations only giving rise to small frequency shifts of the  $\nu_3\text{PO}_2$  mode at about  $1150\text{ cm}^{-1}$ , which increases when smaller cations are replacing larger ones.

In  $\text{AgPO}_3\text{-Ag}_2\text{SO}_4$  glasses, the band at  $965\text{ cm}^{-1}$  can be related to the symmetric  $\text{SO}_4$  mode. At first sight, it seems there are only a superposition of  $\text{PO}_3$  and  $\text{SO}_4$  modes without noticeable interactions between them; in particular, the spectrum of the  $\text{AgPO}_3$  network glass is not modified by  $\text{Ag}_2\text{SO}_4$  addition since only the intensity enhancement of the  $\text{SO}_4$  mode at  $965\text{ cm}^{-1}$  can be observed; there is no modification in the half-width and the frequency of this mode for different  $\text{SO}_4$  ratios (Table I). The areas of the whole  $\text{PO}_2$  and POP bands nearly remain in the same ratio ( $A_{\text{PO}_2}/A_{\text{POP}} \approx 1.2$ ) within the glassy range; however, a sharp analysis of their profiles shows the appearance of a shoulder at  $1135\text{ cm}^{-1}$  within the

$\nu_3\text{PO}_2$  band and an increase of the lower-frequency component ( $675\text{ cm}^{-1}$ ) intensity for the  $\nu_3\text{POP}$  band; the respective areas of the components for these bands are reported in Table I along with their frequencies and half-widths. We are not able, at this time, to give detailed explanations upon these slight perturbations in the structure of  $(\text{PO}_3)_n$  bands. Nevertheless, this description leads to the assumption that the mixed glasses are built with very long  $\text{PO}_3$  chains and  $\text{SO}_4$  groups inserted between them. To confirm this hypothesis, we compared these spectra to those of  $(1-x)\text{AgPO}_3\text{-}x\text{Ag}_2\text{SO}_4$  glasses.

The insertion of  $\text{Ag}_2\text{O}$  in  $\text{AgPO}_3$  glass gives major modifications in the Raman spectra which are already evident for  $x = 0.1$  (Fig. 4). Two new strong lines appear at

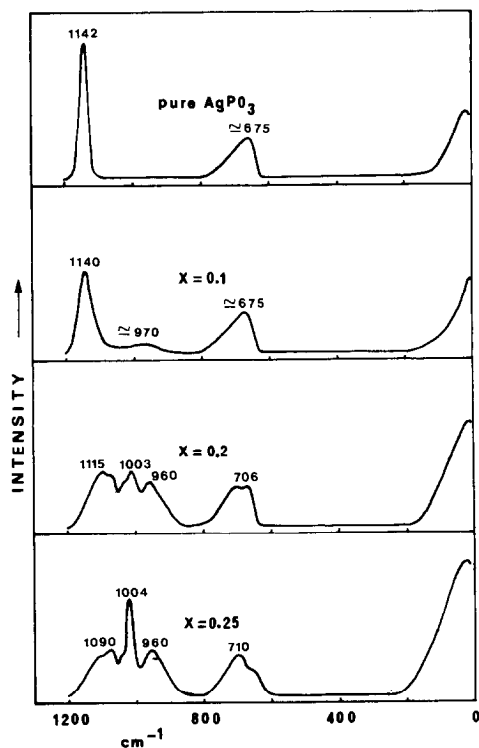


FIG. 4. Raman spectra of  $(1-x)\text{AgPO}_3\text{-}(x)\text{Ag}_2\text{O}$  glasses.

TABLE I  
 FREQUENCIES ( $\bar{\nu}$ ), HALF-WIDTHS ( $\Delta\bar{\nu}_{1/2}$ ), AND AREAS RATIO ( $A_{\nu_1}/A_{\nu_2}$ ) OF THE THREE MAIN RAMAN BANDS IN  $\text{AgPO}_3\text{-Ag}_2\text{SO}_4$  SYSTEM

x	$\nu_3\text{PO}_2$ ( $\text{cm}^{-1}$ )			$\nu_3\text{SO}_4^2$ ( $\text{cm}^{-1}$ )			$\nu_3\text{POP}$ ( $\text{cm}^{-1}$ )			Observations		
	$\nu_1$	$\Delta\bar{\nu}_{1/2}$	$\nu_2$	$A_{\nu_2}/A_{\nu_1}$	$\nu$	$\Delta\bar{\nu}_{1/2}$	$\nu_3$	$\Delta\bar{\nu}_{1/2}$	$\nu_4$		$\Delta\bar{\nu}_{1/2}$	$A_{\nu_3}/A_{\nu_4}$
	0	1139	6								711	7
0	1142	16		0			676	37	708	70	0.625	$\text{AgPO}_3$ glass
0.075	1145	16	1133	0.75	964	20	676	37	707	69	0.71	
0.15	1145	13	1132	0.95	963	20	676	34	708	56	1.08	
0.225	1144	14	1132	1.02	964	20	674	35	706	69	1.25	
0.3	1144	13	1134	1.10	965	19	677	35	710	59	1.40	Vitreous domain limit
0.5	1145	13,5	1134	1.20	968	17	680	36.5	710	56	1.50	Inhomogeneous glass
1					970	12						Polycrystalline $\text{Ag}_2\text{SO}_4$

1004 and 960  $\text{cm}^{-1}$  in these glasses along with the splitting of the clump around 720  $\text{cm}^{-1}$  into two components; the 710- $\text{cm}^{-1}$  one becomes predominant at the limit of the glass homogeneity ( $x = 0.25$ ), which corresponds to the  $\text{Ag}_5\text{P}_3\text{O}_{10}$  formulation.

There are many similarities between the Raman spectra of the  $x = 0.25$  glass and of  $\text{Na}_5\text{P}_3\text{O}_{10}$  crystalline compound that we have recorded. Thus it is clear that short  $\text{P}_3\text{O}_{10}^{5-}$  species are present in this glass, the appearance of shoulders at 1115  $\text{cm}^{-1}$  ( $\nu_s\text{PO}_2$ ) and 690  $\text{cm}^{-1}$  ( $\nu_s\text{POP}$ ) showing that slightly longer chains are mixed with these short ones. The disappearance of the original line at 1145  $\text{cm}^{-1}$ , specific of very long chains, is a good test for their absence and for their breakdown in shorter ones (22). Consequently, the chains are broken when the  $\text{Ag}_2\text{O}$  ratio increases, the formation of  $\text{PO}_3$  terminal groups being easily proved by the appearance of the line at 1004  $\text{cm}^{-1}$  ( $\nu_s\text{PO}_3$ ).

The  $\text{AgPO}_3\text{-Ag}_2\text{SO}_4$  glasses and the  $\text{AgPO}_3\text{-Ag}_2\text{O}$  glasses have very different structural features. We are sure that neither  $\text{P-OSO}_3$  terminal groups nor  $\text{S-O-S}$  or  $\text{P-O-S}$  bridges are present in the glasses.  $\text{SO}_3$  terminal groups are indeed revealed by

a line at 1070  $\text{cm}^{-1}$  (23) and  $\text{SO}_2$  groups give rise to a line at 1270  $\text{cm}^{-1}$  (24) ( $\nu_s\text{SO}_2$ ); none of these modes appears in the Raman spectra.

Thus these  $\text{AgPO}_3\text{-Ag}_2\text{SO}_4$  glasses are built from a network of distorted  $(\text{PO}_3)_n^-$  polyanions, tetrahedral  $\text{SO}_4^{2-}$  ions, and from  $\text{Ag}^+$  cations necessarily coordinated to oxygen atoms of both  $\text{PO}_2$  groups and  $\text{SO}_4$  ions. We could think that the slight modification in the profile of the  $\nu_s\text{PO}_2$  band associated to the appearance of the 1135- $\text{cm}^{-1}$  component results from a distortion of the  $\text{O-Ag}$  interactions.

The profile of the  $\text{SO}_4^{2-}$  ion band at 965  $\text{cm}^{-1}$  is not modified by their concentration in the glass. Its integrated intensity  $A_{\text{SO}_4}$  could be used as an internal standard of  $\text{SO}_4^{2-}$  species concentration since, as shown in Fig. 5, it rises linearly with the  $\text{SO}_4$  concentration. The sum of the areas  $A_{\text{PO}_2}$  and  $A_{\text{POP}}$  is a good standard also of the  $\text{PO}_3$  concentration. We will use this sum, noted  $A_{\text{PO}_3}$ , as the internal reference in the following quantitative study in which we shall explain the variations of the very low frequency band intensity versus the  $\text{Ag}_2\text{SO}_4$  ratio; in particular the  $A_{\text{SO}_4}$  intensity cannot be used for the pure host glass.

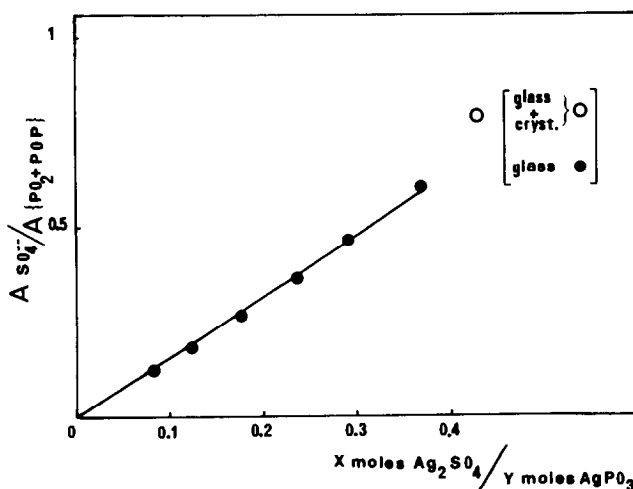


FIG. 5. Linear relationship between the  $\nu_s\text{SO}_4$  band intensity and the molar ratio  $\text{Ag}_2\text{SO}_4/\text{AgPO}_3$ .

#### 4.2. Characteristics of the Low-Frequency Range ( $\bar{\nu} < 200 \text{ cm}^{-1}$ )

The reduced spectra (Ir) below  $200 \text{ cm}^{-1}$  are shown in Fig. 6 with respect to a fixed  $A_{\text{PO}_3}$  value and for different  $\text{Ag}_2\text{SO}_4$  ratios. There is a dissymmetric broad band centered at about  $55 \text{ cm}^{-1}$  and weakly polarized ( $\rho \approx 0.5$ ) and which is not shifted with  $x$  ratio. Its intensity is increasing with the  $\text{Ag}_2\text{SO}_4$  concentration; the area calculations of this band compared with  $A_{\text{PO}_3}$  and  $A_{\text{SO}_4}$  standards allow us to determine that the intensity follows exactly the ratio  $(\text{Ag}^+)/(\text{PO}_3)$ ; when we report in a plot (Fig. 7) the respective areas ( $A_{55 \text{ cm}^{-1}}/A_{\text{PO}_3}$ ) versus the fraction  $(\text{Ag})/(\text{PO}_3)$ , the points are aligned near a straight line. This quantitative correlation is a good proof that the low-frequency band is essentially related to  $\text{Ag}^+$  oscillations in their potential wells.

In  $\text{AgPO}_3\text{-Ag}_2\text{O}$  glasses, the intensity of the observed band remains also nearly con-

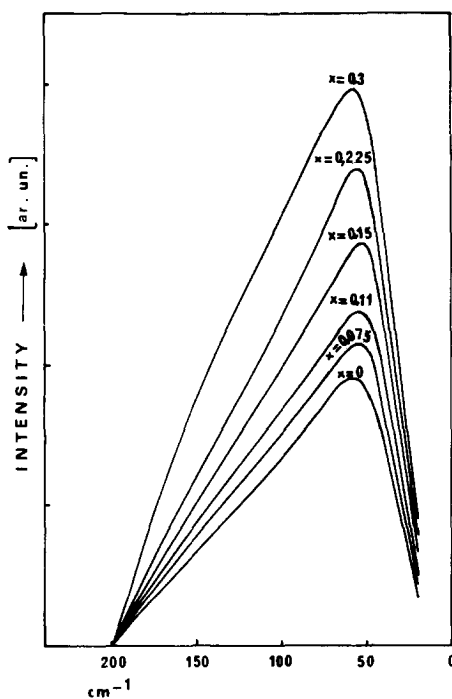


FIG. 6. Low-frequency Raman spectra of  $(1-x)\text{AgPO}_3\text{-}(x)\text{Ag}_2\text{SO}_4$  glasses.

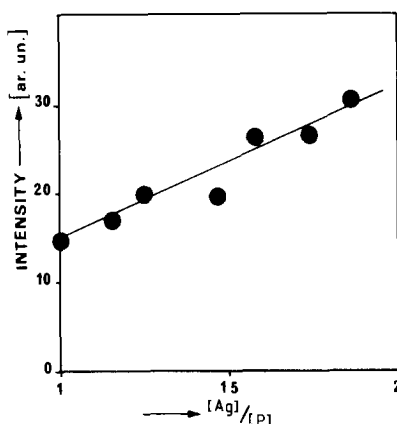


FIG. 7. Linear dependence of the low-frequency Raman band intensity with molar ratio  $\text{Ag/P}$  for  $(1-x)\text{AgPO}_3\text{-}x\text{Ag}_2\text{SO}_4$  glasses.

stant when it is compared to the same  $\text{Ag}^+$  concentration. As we have previously seen, there are short chains in these glasses, so many variations in the spectra would be expected if librational modes of these units were the source of this Raman band.

A qualitative explanation of the assignment of this low-frequency band to cation oscillations rather than to librational modes of the  $\text{PO}_3$  chains will be discussed in a future paper (25), in which the dependence of both frequency and intensity of this band will be discussed with respect to the molar fraction  $\text{Ag/Na}$  in mixed  $(\text{Ag-Na})$  cation phosphate glasses.

#### 4.3. Raman Conclusions

The qualitative and quantitative arguments we are going to expand lead us to think that this low-frequency band reflects oscillation modes of  $\text{Ag}^+$  cations inside their oxygen cages (probably  $\text{AgO}_4$  or  $\text{AgO}_5$ ) and that the attempt-frequency mode lies inside this clump. If we suppose a sinusoidal potential with  $\text{Ag}^+$  sites at a mean distance  $d$ , the activation energy  $E_c$  for a hopping process is given by the relation  $E_c = 2\Pi d^2 \bar{\nu}^2 c^2$  (26). But this  $d$  value is not known, so we may calculate it by a choice of  $\bar{\nu}$  and  $E_c$ ; a mean length jump of  $3 \text{ \AA}$  is

thus obtained with  $\bar{\nu} = 55 \text{ cm}^{-1}$  and  $E_c = 12.7 \text{ kcal} \cdot \text{mole}^{-1}$ , for glassy  $\text{AgPO}_3$ ; it must be noticed that this distance is close to the site-to-site distance between two  $\text{Ag}^+$  sites in  $\text{AgPO}_3$  (17).

As this broad band is not shifted when  $x$  increases, one may suppose that the hopping distance decreases when going from  $\text{AgPO}_3$  pure glass to the saturated  $0.7(\text{AgPO}_3) \cdot 0.3(\text{Ag}_2\text{SO}_4)$  glass. Thus a value of  $2.7 \text{ \AA}$  is obtained for this glass, which seems very realistic.

## 5. Conclusions

Electric measurements and Raman investigations on the vitreous electrolytes  $(1-x)(\text{AgPO}_3) \cdot x\text{Ag}_2\text{SO}_4$  ( $0 < x < 0.3$ ) reveal the following considerations:

—First, the dissolution of  $\text{Ag}_2\text{SO}_4$  in  $\text{AgPO}_3$  glass clearly improves the ionic conductivity properties of the host glass without altering either the electronic conductivity or the redox stability range.

—The ionic conductivity of these mixed glasses is the same as that of the  $\text{AgPO}_3\text{-Ag}_2\text{O}$  glasses when the comparison is made for identical  $[\text{Ag}^+]/[\text{PO}_3^-]$  ratio, though the structures of these two systems are quite different. For  $\text{AgPO}_3\text{-Ag}_2\text{O}$  glasses the chains of the network are broken, the chains shortening versus the  $\text{Ag}_2\text{O}$  concentration, but for  $\text{AgPO}_3\text{-Ag}_2\text{SO}_4$  glasses the network is not modified and the  $\text{SO}_4^{2-}$  ions are probably lying between the chains without interactions with them. In particular, no insertion of  $\text{SO}_4$  group inside the skeleton of a chain occurs.

—The low-frequency band in the Raman spectra is correlated to oscillations of all  $\text{Ag}^+$  cations. The attempt frequency is certainly included in this band and gives rise to a mean length jump going from 3 to  $2.7 \text{ \AA}$  when going from the host  $\text{AgPO}_3$  glass to the saturated  $0.7 \text{ AgPO}_3\text{-}0.3 \text{ Ag}_2\text{SO}_4$  glass.

## References

1. D. KUNZE, in "Fast Ion Transport in Solids" (W. Van Gool, Ed.), p. 405, North-Holland, Amsterdam (1973).
2. J. KUWANO AND M. KATO, *Denki Kagaku* **43**, 734 (1975).
3. M. LAZZARI, B. SCROSATI, AND C. A. VINCENT, *Electrochim. Acta* **22**, 51 (1977).
4. T. MINAMI, H. NAMBU, AND M. TANAKA, *J. Amer. Ceram. Soc.* **60**, 283 (1977).
5. T. MINAMI, H. NAMBU, AND M. TANAKA, *J. Electrochem. Soc.* **124**, 1659 (1977).
6. G. CHIODELLI, A. MAGISTRIS, AND A. SCHIRALDI, *Electrochim. Acta* **23**, 585 (1978).
7. J. P. MALUGANI, A. WASNIEWSKI, M. DOREAU, G. ROBERT, AND A. AL RIKABI, *Mater. Res. Bull.* **13**, 427 (1978).
8. J. P. MALUGANI, A. WASNIEWSKI, M. DOREAU, G. ROBERT, AND R. MERCIER, *Mater. Res. Bull.* **13**, 1009 (1978).
9. J. E. BAUERLE, *J. Phys. Chem. Solids* **30**, 2657 (1969).
10. D. RAVAINÉ AND J. L. SOUQUET, *J. Chim. Phys.* **71**, 693 (1974).
11. C. WAGNER, "Proc. CITCE VII," p. 361 (1955).
12. R. SHUKER AND R. W. GAMMON, *Phys. Rev.* **25**, 222 (1970).
13. R. F. BARTHOLOMEW, *J. Non-cryst. Solids* **12**, 321 (1973).
14. A. ABOU EL ANOUAR, Thesis, Besancon, July 1979.
15. A. KONE, Thesis, Grenoble, June 1980.
16. A. LEVASSEUR, J. C. BRETHOUS, J. M. REAU, P. HAGENMULLER, AND M. COUZI, *Solid State Commun.* **32**, 921 (1979).
17. K. M. JOST, *Acta Crystallogr.* **14**, 779 (1961).
18. YA. S. BOBOVICH, *Opt. Spectrosc.* **13**, 274 (1962).
19. B. N. NELSON AND G. J. EXARHOS, *J. Chem. Phys.* **71**, 2739 (1979).
20. A. BERTOLUZZA, M. A. MORELLI BERTOLUZZA, AND C. FAGNANO, *Lincei. Rend. Sci. Fis. Mat. Nat.*, **54**, 944 (1973).
21. N. H. RAY, *Glass Technol.* **16**, 107 (1975).
22. I. V. FAWCETT, D. A. LONG, AND L. H. TAYLOR, "Proc. V Int. Conf. Raman Spectr., Friburg, 1976," p. 42.
23. R. J. GILLESPIE AND E. A. ROBINSON, *Canad. J. Chem.* **40**, 658 (1962).
24. G. E. WALRAFEN AND T. F. YOUNG, *Trans. Faraday Soc.* **56**, 1419 (1960).
25. R. MERCIER, J. P. MALUGANI, B. FAHYS, AND G. ROBERT, to be published.
26. P. COLOMBAN, R. MERCIER, AND G. LUCAZEAU, *J. Chem. Phys.* **75**, 1388 (1981).